Cyclic fatigue crack propagation behaviour under mode I loading conditions for SiC-Al matrix composites

Yassin L. Nimir
Faculty of Eng., Mu'tah University, Jordan

The mechanisms of fatigue crack growth is studied in the continuous SiC fibre reinforced Al (LM0 and LM25) and unreinforced metal matrix materials, under fully reversed loading R=-1 and zero tension (R=0) cyclic loading for the same values of load amplitude (i.e. Pmax = constant) with particular attention to the effect of compressive and shear stresses on fibre-matrix interactions; where the crack is subjected to mode I loading conditions on a plane perpendicular to the aligned fibres. A series of fatigue tests using pre-cracked Wedge Opening Loaded (W.O.L) specimens were performed to study and monitor the crack growth into such composites. Fatigue Crack Growth (F.C.G) results obtained indicate that SiC-LM0 composites exhibited a superior crack resistance relative to the SiC-LM25 composites under both load ratios and for the same Kmax, Pmax values. Paris constants c and n were also evaluated. Fractographic observations and load vs. displacement curves obtained under R = -1 indicate that the compressive load to the specimen and hence to the crack faces led to crack closure which in turn damaged the pulled out fibres, breaking them in bending and shear. This produced a degradation of the bridging fibres and a reduction in the degree of shielding which they provide. The effect of R ratios on crack growth behaviour in unreinforced matrix materials is the opposite to that observed in the composites, faster growth rates for R = 0 and slower crack growth rates for R = -1, for the same value of Kmax. This reveals that compressive components of load act upon the efficiency of the fibre bridging mechanism.

تم دراسة آلية امتداد (نمو) التصدع تحت الفحوصات الكلالية للمادة المركبة من ألمنيوم (LM 0 & LM 25) المقوى بألياف السيليكون كارباید المستمرة والألمنيوم الغير مقوى – تحت التحميل الدورى المنعكس بالكامل (R=-1) وصفر شد (R=0) تحت نفس القيم من مدى تردد الحمل مع الأنتباه إلى تأثير الإجهادات الضغطية والقصية على الترابط بين الألياف والمعدن عندما يكون التصدع متعرضاً الى ظروف النمط التحميلى الأول على مسطح متعامد على أتجاه الألياف. تم إجراء مجموعة من فحوصات الكلال على عينات تحتوى على تصدعات أسفينية مستحدثة مسبقاً وتم دراسة نمو التصدعات فى هذه العينات المصنوعة من المواد المركبة الأنفة الذكر. نتائج نمو التصدع الكلالى التى تم الحصول عليها فى هذه الدراسة تشير إلى أن المركب المكون من سيليكون كارباید – المنيوم LM0 أظهر تفوقاً على المركب المتكون من سيليكون كارباید– المنيوم LM25 من حيث مقاومة نمو التصدع تحت نفس الظروف التحميلية لكلا المركبين وتم تقييم الثوابت المتعلقة بذلك. وقد أثبتت الفحوصات المجهرية للتصدعات اضافة إلى نتائج منحنيات التحميل ضد الإزاحة تحت ظروف التحميل (R=-1) ان الحمل الضغطى على العينة وعلى مسطحات التصدع ادى الى تسكير التصدع مما أدى بدورة الى تحطيم الألياف المسحوبة والتى تكسرت بسبب الثنى والقص والذى أدى إلى انحطاط فى الياف التجسير وضعف فى درجة الحماية التى تزودها هذه الألياف فى حين أثبتت الدراسة على المعدن غير المسلح عكس ذلك مما يشير ألى ان مركبة الحمل الضغطى تؤثر على فعالية آلية التجسير للألياف.

Keywords: Fatigue crack growth, Crack propagation, Metal matrix composites, Cyclic loading, Fibre bridging

1. Introduction

The growth of cracks under the influence of cyclic loading is a problem of great engineering importance in structural applications involving fibre reinforced metal matrix composites. The process of fatigue failure in theses inhomogeneous materials has proven difficult to explain in fundamental terms. This is due, in part to the fact that there are differences between the fatigue phenomenon in composite materials and the fatigue response of more common structural materials such as aluminium, and titanium. One of these comes about because a single fatigue crack which propagates through a composite component to cause failure, rarely occurs in the singular manner identified with homogenous materials. Instead, fatigue crack growth consists of various combinations of matrix cracking, fibre pullout, void growth, and fibre breakage. As a result, fatigue failure

cannot be defined in terms of a single mode, and a single criterion for fatigue failure is difficult to choose. However, previous work [1, 2, 3], has indicated that many varieties of fibre reinforced matrix materials under monotonic loading conditions behave in a crack-sensitive manner that can be described by the fracture mechanics parameters found useful for homogenous materials. They found that the basic mechanism of crack propagation resistance for these composites, with fibres parallel and perpendicular to the load, was due to crack by the growth of secondary sub-critical cracks perpendicular to the direction of main crack propagation. In addition, they found that the fracture surface work is equivalent to the elastic energy dissipated upon failure of matrix, debonded and pulledout fibres.

The fracture resistance of fibre reinforced Metal Matrix Composites (MMC's) under cyclic loads is a subject of considerable scientific and engineering interest. Despite the need for a clear understanding of the fatigue crack growth behaviour of MMC's for a variety of potential structural applications, little attention has thus far been devoted to this area of research.

Recent studies [4, 5], reported that fatigue behaviour is controlled by crack nucleation and not crack growth. In these studies, positive values of the stress ratio (R) have invariably been used on smooth and precracked specimens and the role of far-field compressive stress has been consistently neglected. Compressive loads and crack closure effects are important in cyclic fatigue not only in ductile metals [6, 7], but also in brittle materials [8, 9].

In this paper, fatigue crack growth behaviour under R = -1, R = 0, cyclic loading, are investigated in precracked Wedge Opening Loaded (WOL) specimens of continuous fibre reinforced and unreinforced Al- 7 wt.% Si- 0.5 wt.% Mg alloy (LM25) and commercially pure 99.9% aluminium matrix materials mode $I_{\perp}$ (i.e. where the crack is perpendicular to the fibre axis).

2. Experimental work

The composite materials employed in this study (in the as fabricated conditions) were made from unidirectionally infiltrated LM25 and LM0 into preforms of continuous Silicon Carbide (SiC) fibres, with a nominal fibre diameter of 12 μm and fibre volume fraction of 45% and 38%, respectively. Their macroscopic mechanical properties are listed in table 1. The mechanical properties of Al(LM25) and Al (LM0) matrix materials are listed in table 2. The fatigue test specimens geometry were dictated by the size and quantity of material plates available. Therefore, the type of specimens and geometry used were a wedge opening loaded specimens (WOL) with height ratio of H/w = 0.486, [10], as shown in fig. 1 and table 3. The tested specimens were machined using a diamond saw in order to have the notch and crack perpendicular ($I_{\perp}$) to the fibre direction. Cyclic fatigue loading tests were carried out at room temperature in a well aligned Schenck servo-hydraulic fatigue machine. In order to maintain good alignment and impose rigidity during tension-compression tests, the specimens were glued in position to the loading pins with epoxy resin while a small tensile load was applied. The cyclic tests were performed at a frequency of 5 Hz with a sinusoidal loading cycle at maintained constant loading range (i.e. Pmax - Pmin = constant) during experiments.

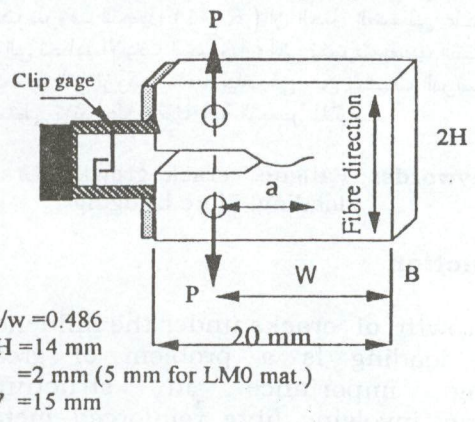

Fig. 1. Wedge opening length specimen configuation used in the fatigue crack growth experiments with the crack being perpendicular to fibre direction, mode $I_{\perp}$.

A pre-selected load range (Pmax) was chosen for each experiment, and tests were started with a small compressive component. The load was then slowly biased towards tension, while the load range remained constant until slow crack growth was detected. Guided by previous experience, it was possible to choose a load range such that the crack could be grown under a load ratio R = Pmin / Pmax = -1 (fully reversed tension-compression cyclic loading). The cyclic fatigue loading tests carried out at R = 0 (zero tension with Pmax = constant throughout the experiments by removing or increasing the compressive load Pmin to zero). Cyclic loading tests were also performed to investigate the effect of far field compressive loads on fatigue crack growth by starting the fatigue tests at a load ratio R = -1 and after a pre-selected crack length had been reached, the compressive load Pmin was increased to near zero value to produce an R ratio equal to zero (tension- tension) till specimen(s) failure occurred.

Table 1
Macroscopic mechanical properties of nicalon fibre reinforced aluminium matrix materials obtained from [11], and compared with values from, [12]

Composite Material	Young's Modulus (GPa)		Tensile Strength (MPa)		Strain to Failure %
	E_{II}	$E_{\perp}$	σ_{II}	$\sigma_{\perp}$	
45% v/o SiC/Al (LM25)	127.635	100.33	1026.1	63.682	-
	128*	-	350*	-	0.27
38% v/o SiC/Al (LM0)	116.64	90.44	897.78	21.01	-
	115*	-	-	-	1

Table 2
Mechanical properties of Al(LM25) and Al(LM0) matrix materials

Material	Tensile stress (MPa)	Yield stress (MPa)	Strain to failure %	$\sigma_{comp.}$ (MPa)	$E_{tensile}$ (GPa)	$E_{comp.}$ (GPa)	Shear modulus (GPa)
Al(LM25) Al-7Si 0.5 Mg	283-262	214-227	3-5	193-220	71.7	72.4	26.8
Al(LM0) Commercially Pure 99.9% Al.	80-90	55-60	15-20	58	72	-	-

Table 3
Wedge opening length (WOL) specimens dimensions used in the monotonic crack growth experiments.

Materials	Height 2H (mm)	Width W (mm)	H / W	Thickness B (mm)	Notch lengths (a / W)
45% v/o SiC/Al (LM25)	14.6	15.0	0.486	2 ± 0.10	0.25 & 0.35
Al (LM25) matrix	14.6	15.0	0.486	2 ± 0.10	0.2
38% v/o SiC/Al (LM0)	14.6	15.0	0.486	3 ± 0.10	0.2 & 0.35
Al (LM0) matrix	14.6	15.0	0.486	5 ± 0.10	0.2

Crack lengths were measured on the polished specimens surfaces to an accuracy of ±0.01 mm using a travelling microscope. The cyclic crack growth rates (da/dN) was determined from the raw data at each measurement of crack growth recorded. The stress intensity factor (K_I), with a constant load and increasing crack length, for the WOL specimen geometry was calculated using a published data in [10]. The stress intensity factor is given by $K_I = \frac{P}{B\sqrt{w}} f\left(\frac{a}{w}\right)$, where P is the maximum applied load, W is the width, and B is the thickness of specimen.

The variation of K_I as a function of the normalized crack length, a/w, is shown in fig. 2. However, only in the case of unreinforced LM0 matrix material, where plastic deformation regions were observed to occur at and ahead of the crack tip, the crack length used in the calculation of K_I values is the crack length corrected for plastic zone $(a + r_y)$, where

$$r_y = \frac{1}{2\pi}\left(\frac{K_I}{\sigma_y}\right)^2 = \frac{a}{2}\left(\frac{\sigma}{\sigma_y}\right)^2$$

and σ_y is the yield stress of the matrix material.

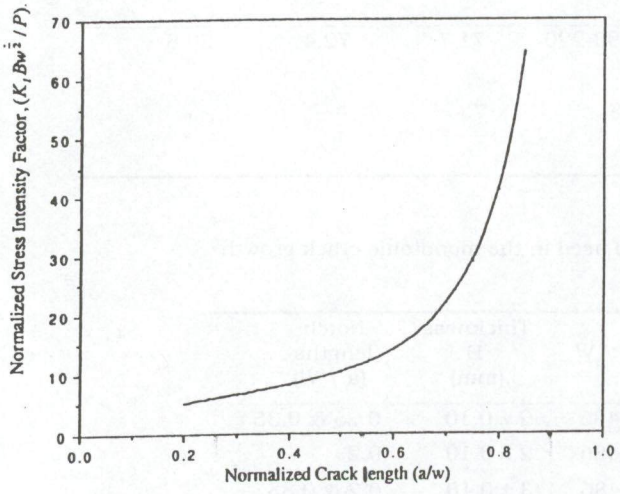

Fig. 2. Variation of normalized stress intensity factor with normalized crack length.

For cyclic loading tests of R = -1 and R = 0, a clip gauge transducer was attached at the front face of the specimen in order to measure the notch opening displacement with a resolution better than 1 μm. The load-displacement curves were obtained at intervals during the tests at the slower frequency of 0.1 Hz.

The fractured surfaces were examined under the Scanning Electron Microscope (SEM) after gold coating, for features, which may explain the fatigue failure behaviour or mechanism.

3. Results and discussion

3.1. Crack propagation characteristics

The results obtained for SiC/LM25 and LM0 composites mode $I_\perp$ are shown in fig. 3 as crack length (a) versus the number of fatigue cycles, N, for R=-1 and R =0.

The results show that once the crack started to propagate under cyclic loading of R=-1 (i.e. with compressive component) it advanced continuously in both composite materials and increased steadily with increasing crack length as the peak stress intensity of the crack tip increased without any cessation of growth. However, under cyclic loading of R = 0, much slower crack growths were observed in both composites for the same value of Kmax. It is also evident from fig. 3 that the crack growth behaviour of SiC/LM0 composite is significantly slower than that of SiC-LM25 composite under R = -1 and importantly under cyclic loading of R = 0 for the same value of Kmax, which is in agreement with the higher value of K_C obtained in [2, 13].

The effect of far field compressive loads on crack growth behaviour on both composites, mode $I_\perp$, can be seen in the results shown in figs. 3 and 4 for cyclic fatigue tests carried out at load ratios of R = -1 and R = 0 in the same specimen. It is interesting to note that when the load ratio R is changed during the tests, at a pre-selected crack length, from R = -1 to R = 0 with the same value of Pmax, the Crack Growth Rate (CGR) is seen to decrease. The high crack growth rate associated with

tension- compression cycling period may be related directly to the effect of crack-faces closure during the unloading and subsequent loading of the specimen(s).

In the case of unreinforced Al matrix materials, the effect of R ratio on crack growth rate is the opposite to that observed in the composites, fig. 4. Faster crack growth rate for R = 0, and slower crack growth rate for R = -1 (i.e. with compressive component), for the same value of Kmax. This reveals that the compressive components of load act upon the efficiency of the fibre bridging mechanism.

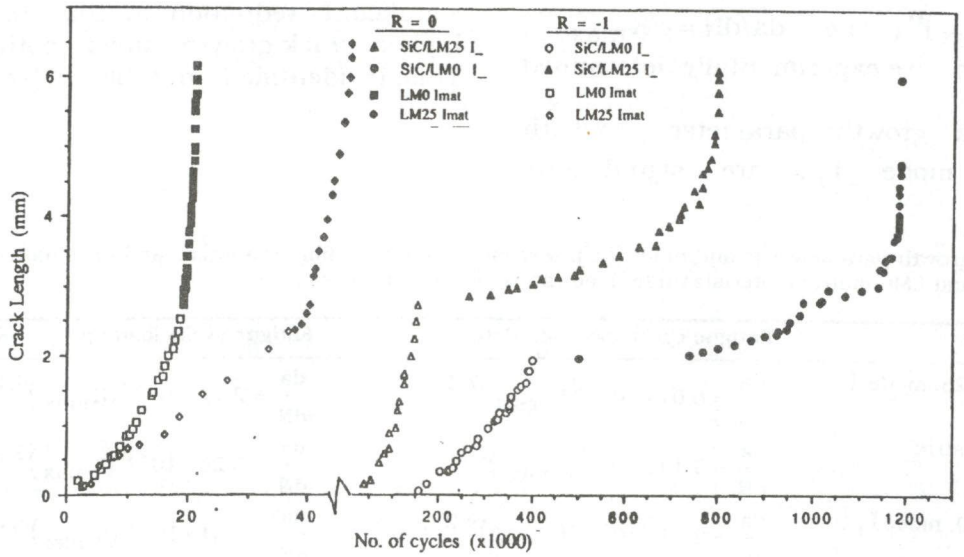

Fig. 3. Crack length versus the number of fatigue cycles under R = -1 and R = 0 for SiC/LM25 and SiC/LM0 composites and for LM25 and LM 0 matrix materials, mode $I_{\perp}$, f = 5 Hz.

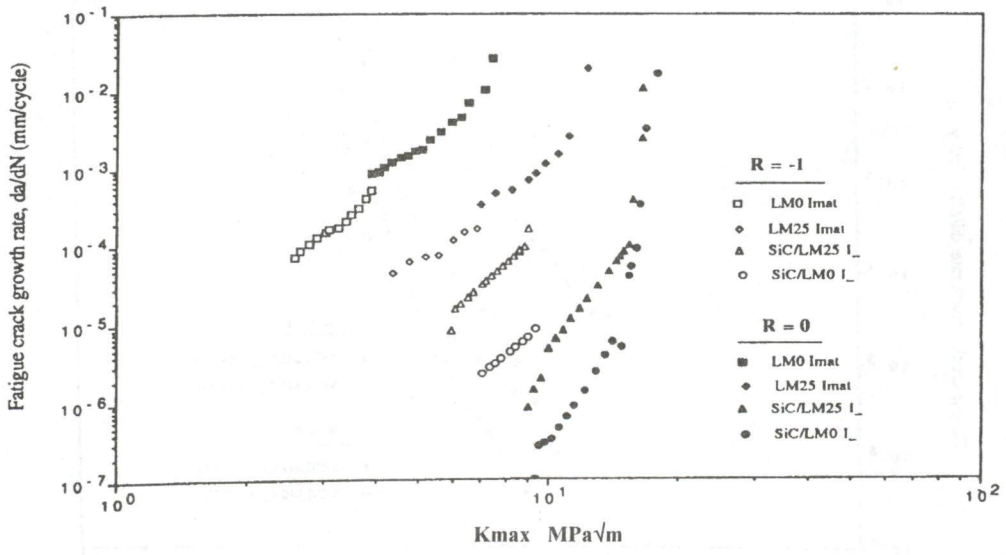

Fig. 4. Fatigue crack growth rate versus the peak stress intensity factor, Kmax for SiC/LM25 and SiC/LM0 composites and LM25 and LM0 matrix materials under R = -1 and R = 0, mode $I_{\perp}$, f = 5 Hz.

Using the data from experiments performed as described, the increment of crack length per cycle, da/dN, was plotted as a function of Kmax in double logarithmic coordinates, fig. 5 and fig. 6. The straight line of the logarithmic plot shows the crack rate to have a power-law dependency on the peak stress intensity factor of the form $da/dN \propto (K_{max})^n$, i.e. $da/dN = c(K_{max})^n$, were c and n are experimentally determined constants.

The crack growth parameter for both composites, mode $I_\perp$, are significantly different (i.e. c is decreased and n is increased) compared to that of Al matrix materials, as shown in table 4. This resulted in a substantial increase in time to failure and slower crack growth for the same values of Kmax. However, it is also important to note that the presence of far-field compressive loads during R= -1 cyclic periods has led to a significant reduction in time to failure and higher crack growth rates in both composites. This is identified in table 4 by the reduced

Table 4
Crack growth parameters (c and n) for the power law function for fibre reinforced and unreinforced LM25 and LM0 matrix materials under load ratios of R = 0 and R = -1

Material	Fatigue cyclic loading, R=0.	Fatigue cyclic loading, R = -1.
SiC/LM25, mode $I_\perp$.	$\frac{da}{dN} = 6.01\times10^{-12}(K_{max})^{7.1}$	$\frac{da}{dN} = 2.12\times10^{-9}(K_{max})^{5.11}$
LM25 Matrix	$\frac{da}{dN} = 8.14\times10^{-7}(K_{max})^{3.2}$	$\frac{da}{dN} = 8.26\times10^{-8}(K_{max})^{3.92}$
SiC/LM0, mode $I_\perp$.	$\frac{da}{dN} = 2.41\times10^{-15}(K_{max})^{9.27}$	$\frac{da}{dN} = 6.51\times10^{-9}(K_{max})^{5.15}$
LM0 Matrix	$\frac{da}{dN} = 9.95\times10^{-6}(K_{max})^{3.43}$	$\frac{da}{dN} = 1.57\times10^{-6}(K_{max})^{3.97}$

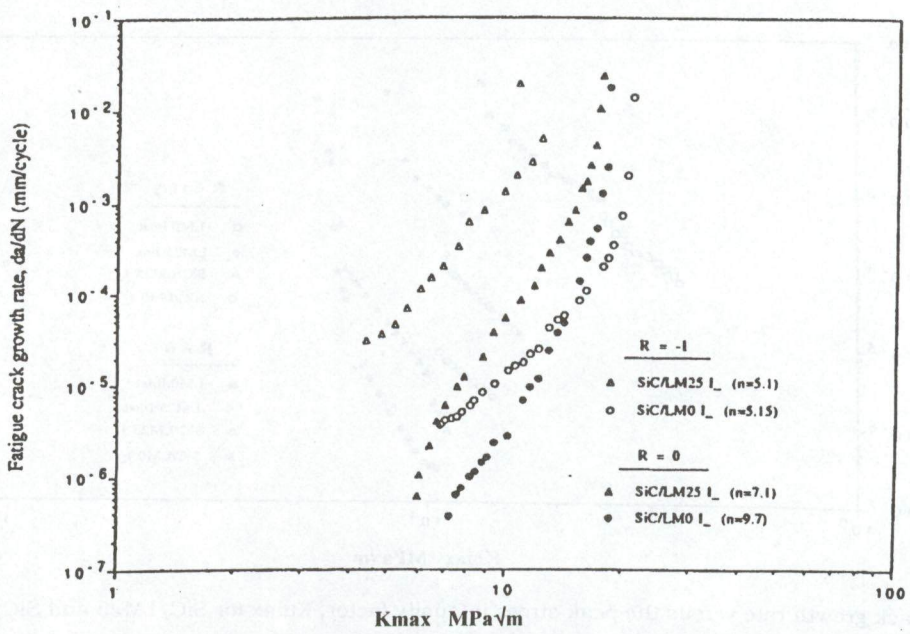

Fig. 5. Fatigue crack growth rate versus the peak stress intensity factor, Kmax for SiC/LM25 and SiC/LM0 composites under R = -1 and R = 0, f = 5 Hz..

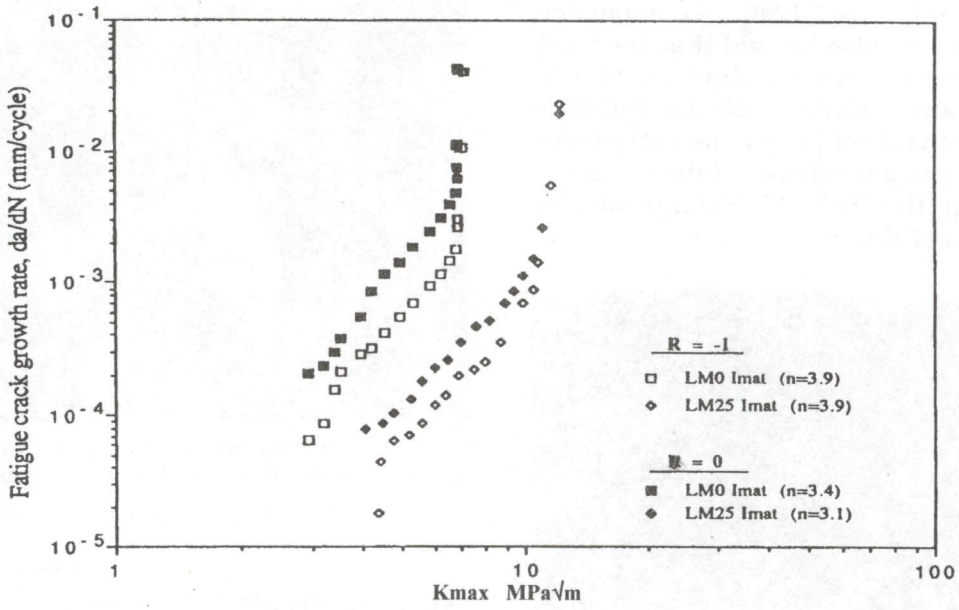

Fig. 6. Fatigue crack growth rate versus the peak stress intensity factor, Kmax for LM25 and LM0 matrix materials under R = -1 and R = 0, mode $I_{\perp}$, f = 5 Hz.

values of n and the increase in c values, in comparison with n and c values under R= 0 cyclic tests. This indicates that the applied compressive load to the specimens and hence to the crack faces has damaged the pulled out fibres that cannot slip back. This produces a degradation of the bridging fibres and a dramatic reduction in the degree of shielding which they provide.

The Paris law growth exponent (n) has been reported to be as high as 14 in previous studies, [14, 15], on SiC reinforced Al- matrix. This is much higher than that of the typical ductile metallic alloys (were n is around 3 to 4) [16].

3.2. Mechanics of crack growth in SiC- LM25 and LM0 composites

3.2.1. Fractography

SEM micrographs of fatigue fracture surfaces at positions which correspond to crack length of a/w of 0.43 and 0.42 for SiC-LM25 and LM0 composites (mode $I_{\perp}$) and corresponding to the fatigue tests with R=0 are shown in fig. 7 (a and b) and fig. 8, respectively. A planar fracture surface was observed to be a common feature over most areas of the fracture surfaces. Little fibre pullout from the matrix and little matrix cracking could be detected for SiC-LM25 composite. Fig. 8 shows that the fracture surface for SiC-LM0 composite was rougher than that of SiC-LM25 composite. It has many pulled out and debonded fibres, causing matrix cracking possibly due to interfacial separation. This together with evidence of some matrix ductility (in rich matrix areas) and possibly localized necking of the matrix between fibres at the fracture surfaces are illustrated in both figs. 7 and 8.

It is interesting to note that the fibre fracture surfaces were smooth in both composites. This is an indication that the fibres have failed or fractured in a tensile mode, and there was no closure or contact of fracture surfaces during the loading or unloading part of the cycle in R = 0 cyclic tests. The little pullout and fibre debonding in the SiC-LM25 composite indicates that fibre-matrix interface strength is higher than in the SiC-LM0 composites. This is consistent with the results obtained by Trumper and Scot, [17], were values of 150 MPa and 30 MPa were reported for the interfacial shear strength of

SiC-LM25 and SiC-LM0 composites, respectively. It can also be said that the weak bond which exists between fibre- matrix and the higher matrix ductility of the SiC-LM0 composite is capable of producing more crack blunting and hence slower fatigue crack growth than in the SiC-LM25 composite, for the same values of Kmax.

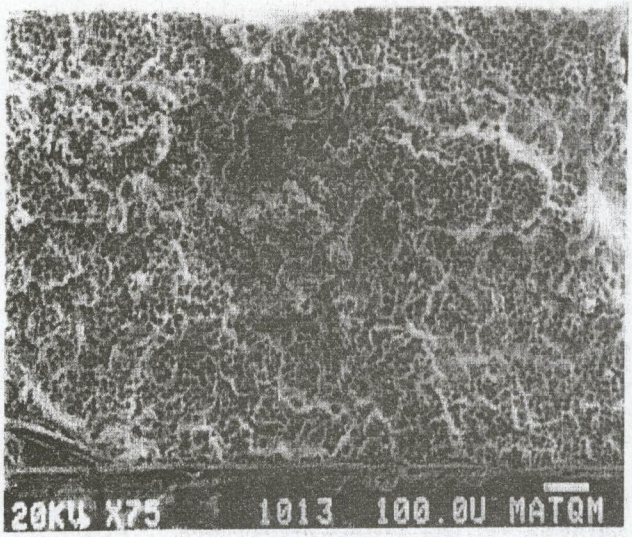

(a)

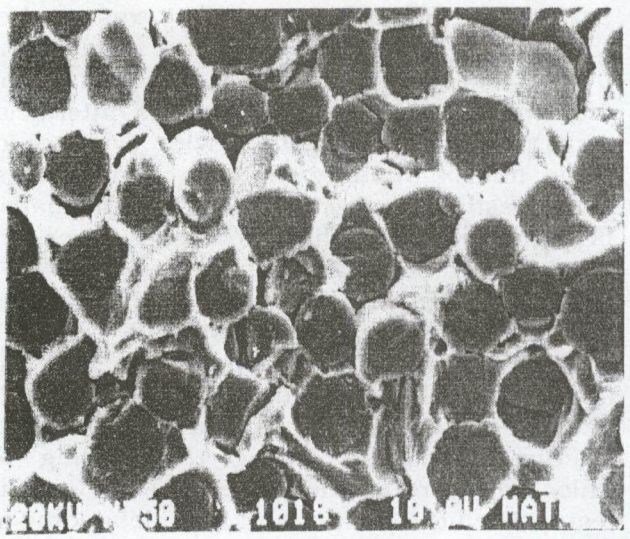

(b)

Fig. 7. (a) SEM micrographs of fatigue fracture surfaces for SiC-LM25 composite resulting from cyclic loading in mode $I_{\perp}$ with R = 0, f = 5 Hz, a/w = 0.43. (b) Higher magnification of (a).

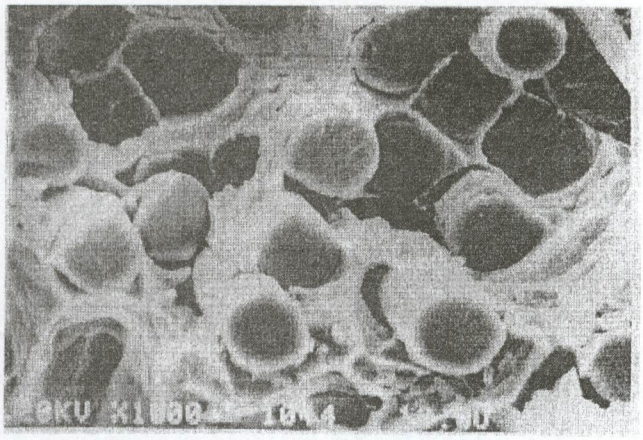

Fig. 8. SEM micrograph showing fracture surfaces at higher magnification for SiC-LM0 composite resulting from cyclic loading in mode $I_{\perp}$ with R = 0, f = 5 Hz, a/w = 0.42.

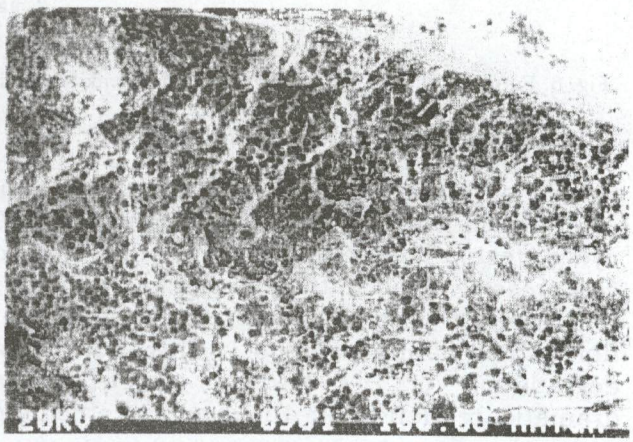

(a)

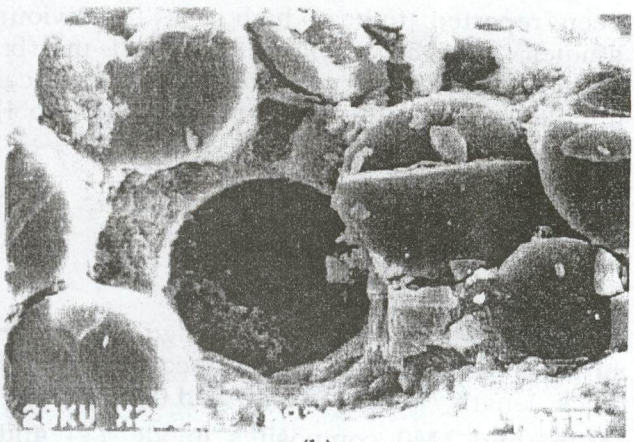

(b)

Fig. 9. (a) SEM micrographs showing fatigue fracture surfaces for SiC-LM25 composite resulting from cyclic loading in mode $I_{\perp}$ with R = -1, f = 5 Hz, a/w = 0.44. (b) Higher magnification of (a).

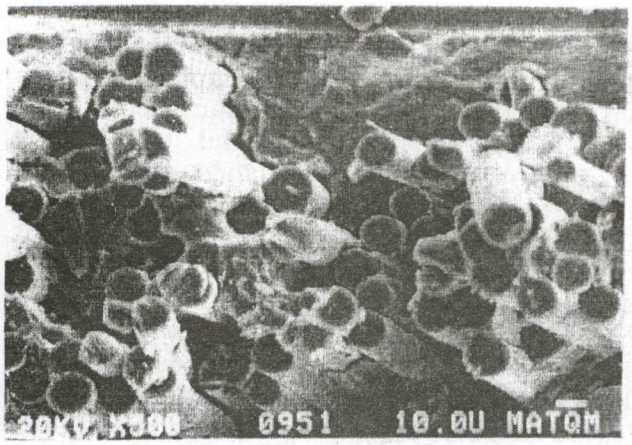

(a)

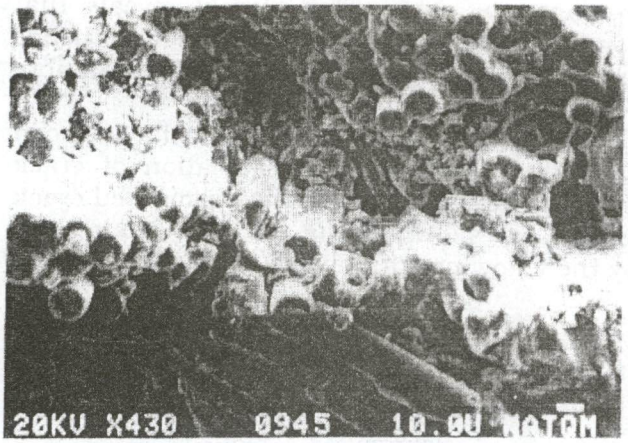

(b)

(c)

Fig. 10. (a) SEM micrographs showing fatigue fracture surfaces for SiC-LM0 composite resulting from cyclic loading in mode $I_{\perp}$ with R = -1, f = 5 Hz, at a = 0.2 mm from notch. (b) with a = 5 mm from notch. (c) Higher magnification of (b).

Examinations of SEM micrographs of fatigued fracture surfaces taken at crack length of 0.44 mm and 0.5 mm from notch for SiC-LM25 and LM0 (mode $I_{\perp}$) corresponding to R = -1 fatigue cyclic tests are shown in fig. 9-a,b and fig. 10-a, b, c, respectively. These results revealed slightly rougher fracture surface than in R = 0 fracture surface. This is shown in facets with step like structure. Evidence of matrix cracking along fibre-matrix interface, some fibre pullout and extensive matrix deformation can also be observed.

The effect of far field compressive load part of the cycle on fracture crack surfaces can be seen at higher magnification in fig. 9-b and fig. 10-c, through the presence of fibre debris, broken fibres and fibre(s) surface damage on these surfaces. This indicates that the applied far field compressive loads to the specimens and hence to the crack faces led to crack closure which in turn damaged the pulled out fibres (that cannot slip back) breaking them in bending and shear. This produced a degradation of the bridging fibres and a reduction in the degree of shielding which they provided.

3.2.2. Crack closure at load ratios of R = 0 and R = -1 for SiC-LM25 and LM0 Composites, mode $I_{\perp}$

Since the mechanisms for cyclic growth in ceramic- metal composites are not well understood, it would be unwise to speculate on how the residual stress produced on closure might affect crack growth rates. However, it is possible to appreciate that, in our experiments, where external compressive loads are applied to the specimens and hence to the crack faces, the presence of crushed and broken fibres can be far more damaging and important.

The load- displacement records taken for SiC- LM0 and LM25 composites, mode $I_{\perp}$, during R = -1 cyclic tests, show the loops to be irreversible on crack closing and opening, fig. 11-a, b. This means that crack faces do not match when the load is reversed because the presence of broken and crushed fibres in the wake of crack prevents crack closure, and hence certain compressive load is needed to

close (at least partly) the crack. The nonlinear constitutive response observed in the loops must be due to either fibre- matrix interfacial degradation or induced plastic deformation capability of the matrix due to the constraining influence of the fibres. The interfacial degradation mechanism appears to be most probable of the two potential mechanisms because gradual softening occurs throughout the fatigue tests. In both composites and immediately after the crack was initiated, it was found that the crack closure load (i.e. the inflection point of the loading curve in the hysteresis loop) decreases with increasing in crack length, that is with increase in the effective stress intensity factor responsible for crack growth.

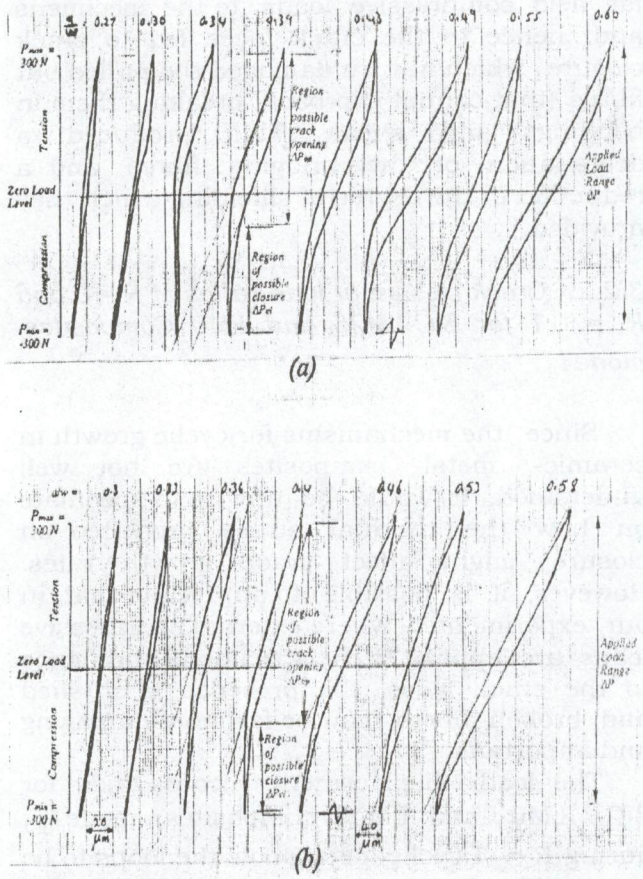

Fig. 11. Schematic representation of load vs. displacement records obtained at various crack lengths under R = -1 cyclic periods, mode $I_{\perp}$, for (a) SiC- LM0 composite, (b) SiC- LM25 composite.

The results indicate that the decrease in closure load for SiC- LM0 composite is less than that of SiC- LM25 composite. It is possible that at a certain crack length the application of compressive load to the crack faces has caused the crushed and broken fibres to be embedded in the highly ductile LM0 matrix material. This resulted in an extensive matrix deformation and higher crack closure load in the next tension- compression cycles to occur. Further damage is induced on the pulled out fibres and fibre surfaces and thus producing a dramatic reduction in the degree of shielding which the bridging fibres provide and hence increasing the crack propagation rates. This clearly reveals that compressive components of load and hence crack closure act upon the efficiency of fibre bridging mechanism.

This type of crack closure behaviour can also be shown by the variation of crack opening ratio, Uop, with the normalized crack length, as shown in fig. 12, and Uop is given by the following equation;

$$U_{op} = \frac{\Delta P_{op}}{\Delta P_{app}} .$$

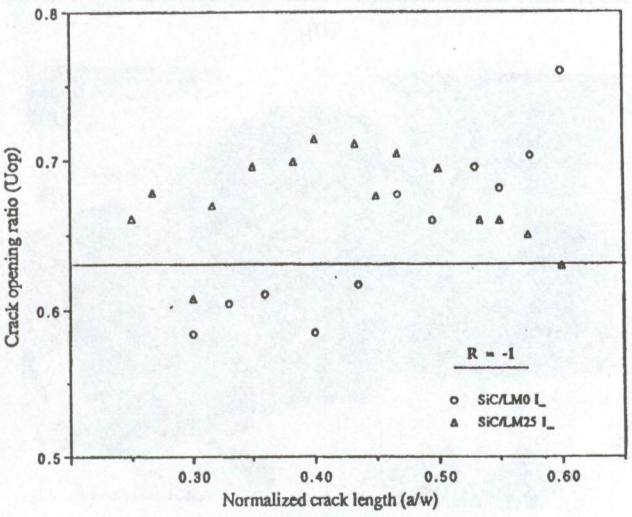

Fig. 12. Variation of crack opening ratio with normalized crack length.

In the above equation, ΔP_{op} is the load opening point and ΔP_{app} represent the applied load range. The crack opening ratio,

Uop, for SiC- LM25 composite increase from the initial value of 0.66 to the value of 0.73 at crack length of a /w = 0.43, and then decreased to the value of 0.63 at the end of the test. Similarly, the crack opening ratio in the case of SiC- LM0 composite, increased from an initial value of 0.5 immediately after crack extension to the value of 0.76 at the end of the test. This means that the effect of ΔK (the stress intensity factor range) on the behaviour of U_{op} under R = -1 can be observed in the range of crack length up to a/w = 0.5.

The load- displacement records taken for SiC- LM0 and LM25 composites, mode $I_{\perp}$, during R = 0 cyclic test are shown in fig. 13 -a, b. This figure shows that the loops close at zero load. This, however, does not mean that the crack closes reversibly. It has a residual opening at zero load which is not shown in the loop. However, the presence of smooth fibre fracture surfaces and undamaged pulled out fibres observed on the fracture surfaces of both composites during SEM investigation (section 3. 1). This indicates that fibres has failed in a tensile mode and there was no closure or contact of fracture surfaces during the loading or unloading part of the cycle in R = 0 cyclic tests. In this case, it is possible to suggest that the crack shielding mechanism which the bridging fibres provide is most effective and the composites have lower fatigue crack growth rates than that under R = -1 cyclic loading. It can also be said that in these figures the effective stress intensity responsible for crack growth during R = -1 is almost equal to the applied Kmax, while at R = 0, it is less than Kmax.

The present observations on the effect of R ratio in the unreinforced Al matrices are in general agreement with the observations reported by Jono and Song [18], on 7075- T6 and 6063- T6 Al alloys, in that crack growth rates increase with increasing stress ratio, R. The load- displacement records obtained under R = -1 cyclic ratio, fig. 14-a, b, show the loops to be irreversible on crack closing and opening in both matrix materials. In this case, it was found that closure load increases with increasing in crack length up to a/w = 0.47, that is with decrease in Keff responsible for crack growth, where,

$$K_{eff} = \left(\Delta P_{op} / B\sqrt{w}\right) f(a/w).$$

Thereafter, the closure load decreases rapidly to near and below zero load level till final failure of specimen.

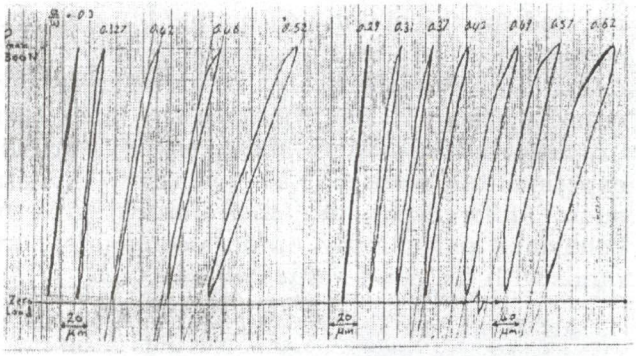

(a) (b)

Fig. 13. Schematic representation of load vs. displacement records obtained at various crack lengths in mode $I_{\perp}$, under R = 0 load ratio for (a) SiC- LM25 composite, (b) SiC- LM0 composite.

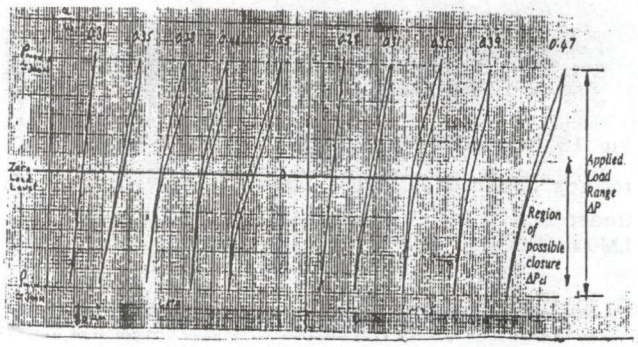

(a) (b)

Fig. 14. Schematic representation of load vs. displacement records obtained at various crack lengths in mode $I_{\perp}$, under R = -1 load ratio for (a) LM25 matrix material, (b) LM0 matrix material.

At R = 0 cyclic tests, fig. 15-a, b shows that the loops close at zero load (i.e. no closure effect), and in this case as would be expected, the effective stress intensity factor, Keff, for crack growth is equal to Kmax. This is consistent with observations reported by Jono and Song, [18], on 2024- T3 Al alloy, in that

crack closure loads decreases with increase in R, hence increasing the effective stress intensity at crack tip resulting in higher crack growth rates. It was interesting to note that the increase in crack closure loads for LM25 matrix materials were surprisingly greater than that of the more ductile LM0 matrix materials. This may indicate that fatigue crack growth behaviour in metals is not only affected by the materials ductility but also the composition of such materials, making it difficult to compare any differences in the crack growth behaviour of the two unreinforced Al matrices. Further experimental work may be required to explain such differences in their crack growth behaviour particularly under decreasing load ratios with the same values of Kmax.

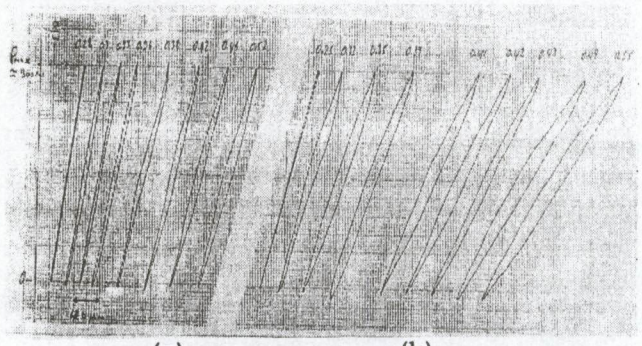

(a) (b)

Fig. 15. Schematic representation of load vs. displacement records obtained at various crack lengths in mode $I_{\perp}$, under R = 0 load ratio for (a) LM25 matrix material, (b) LM0 matrix material.

4. Conclusions

Fatigue crack growth and growth rates were investigated on both reinforced and unreinforced LM0 and LM25 matrix materials for the same value of Kmax and under various (R) loading ratios. An emphasis was made on determining the governing mechanical parameters for crack growth behaviour including that of fibre bridged cracks, using load vs. displacement records obtained under both loading ratios. The main results are summarized as follows:

1- Fatigue cycling with fully reversed (R = -1) conditions, produces faster crack growth rates in both composites, mode $I_{\perp}$, than with load ratio of R = 0. However, the effect of R ratios on crack growth behaviour in unreinforced matrix materials is the opposite to that observed in the composite for the same value of Kmax. This indicates that the compressive component of load act upon the efficiency of the fibre bridging mechanism.

2- Composites with ductile matrix and low fibre- matrix interfacial strength SiC/LM0 composites, showed superior crack growth resistance relative to the high fibre- matrix interfacial strength and more brittle matrix materials systems (SiC/LM25 composite) under both load ratios and for the same Kmax values. The fatigue crack growth data obtained for both reinforced and unreinforced matrix materials revealed a power law relationship between the peak stress intensity factor (Kmax) and crack growth rates.

3- The results obtained and fractographic observations for both composites under R = 0 cyclic load show that the increase in crack resistance is mainly due to crack bridging by the fibres. This can be considered as a potential shielding mechanism that could effect fatigue crack growth resistance. The presence of broken fibres, fibre debris and fibre surface damage on the fracture surfaces under R = -1 loading conditions clearly indicates that the applied far- field compressive load of the cycle to the specimen and hence to the crack faces led to crack closure which in turn damage the pulled out fibres, breaking them in bending and shear. This produces a degradation of the bridging fibres and a reduction in the degree of shielding which they provide. Furthermore, the acceleration and deceleration of fatigue crack growth at both load ratios were explained in terms of ΔKeff, and it was concluded that ΔKeff is an important parameter for controlling the fatigue crack growth of bridged cracks.

Nomenclature

P	Applied load range,
R	Cyclic loading ratio,
da/dN	Cyclic crack growth rate,
K_I	Stress Intensity Factor,

B	Thickness of specimen,
W	Width of specimen,
a/w	Normalized crack length,
a	Crack length,
σ_y	Yield Stress,
r_y	Correction factor for plastic zone,
N	Number of fatigue cycles,
K_{max}	Peak Stress Intensity Factor,
f	Frequency,
c, n	Experimentally determined constants,
U_{op}	Crack opening ratio,
ΔP_{op}	Load opening point,
ΔP_{app}	Applied load range, and
ΔK	Stress intensity factor range.

Acknowledgements

The author is indebted to Dr. Ramadan J. Mustafa for his assistance. The author is grateful for the cooperation of the staff at the mechanical engineering labs at Mu'tah University and Sussex University in addition to Dr. Ismail Al-Raheil for his help in using the SEM.

References.

[1] D. F. Hasson, C. R. Crowe, J. S. Ahearn, and D. C. Cooke, Failure mechanisms in high performance materials, ed. Early, Shiversand Smith, Cambridge Univ. Press (1985).

[2] S. J. Harris and T. E. Wilks, Fatigue crack growth in discontinuous fibre reinforced aluminium alloys, Sixth International Conference on Composite Materials, ICCM & ECCM, Vol.2, edt. J. Morton, Applied Science Pub., New York, pp. 2.113-2.123 (1989).

[3] W. R. Hoover, Crack initiation in B- Al composites, J. Comp. Mat., Vol. 10, pp. 106 (1976).

[4] W. S. Johson, and R. R. Wallis, Fatigue behaviour of continuous fibre Silicon Carbide / Aluminium composites, Composite Materials: Fatigue and Fracture, ASTM STP 907, H.T. Hahn, Ed., American Society for Testing and Materials.

[5] J. T. Evans, Fracture and sub-critical crack growth in Alumina Fibre reinforced Magnesium composites, Acta. Metall., Vol. 34 (10), pp. 2075-2083 (1986).

[6] T. Christman, and S. Surresh, Engineering Fracture Mechanics, Vol. 23, pp. 953- (1986).

[7] L. E. Wart, and S. Surresh, Crack propagation in ceramics under cyclic loads, J. Mater. Sci., Vol. 22, pp. 1173-1192 (1987).

[8] M. S. Ashby, and S. P. Hallam, Acta. Metall., Vol. 34, p. 497 (1986).

[9] C. J. Beevers, K. Bell, and E. A. Stark, A model for fatigue crack closure, Eng. Fract. Mech., Vol. 19 (1), pp. 93- 100 (1984).

[10] A. Saxena, and S. J. Hudak, Jr., Review and extension of compliance information for common crack growth specimens, Int. J. Fract., Vol. 14 (5), pp. 453-467 (1978).

[11] J. Hull, An introduction to composite materials, Cambridge University Press, New York (1981).

[12] A. R. Skinner, The effect of heat transfer on the mechanical properties and microstructure of Aluminium alloy MMC's, Metal Matrix Composites, 2nd. Conference, Nov. (1989).

[13] R. J. Mustafa, and F. Guiu, Fatigue of continuous fibre reinforced Aluminium Matrix Composites, Metal Matrix Composites, VI, The Royal Society, U.K., 26- 27 Nov. (1997).

[14] C. M. Friend, J. Material Sci., Vol. 5, pp.1- 7 (1989).

[15] W. A. Logsdon, and P. K. Liaw, Tensile fracture toughness and fatigue crack growth rate properties of Silicon Carbide whiskers, or particulate reinforced aluminium metal matrix composites, Scientific Paper 83- ID7- NODEM. P1, Westinghouse R and D Centre, Pittsburgh, Pa, Dec. (1983).

[16] American Society for Metals, Properties and Selection: Nonferrous alloy and pure metals, Metals Handbook, 9th. Edition, Vol. 2, pp. 63-161 (1979).

[17] R. L. Trumper, and V. D. Scott, Cast Microstructures in fibre reinforced metals, 7th. International Conference on the Materials Revolution through the 90's, p. 27 (1989).

[18] M. Jono, and J. Song, Growth and closure of short fatigue cracks, recent advances in composites in the U.S and Japan, ASTM STP 864, edited by J. R. Vinson and M. Taya, pp. 41- 65 (1985).

[19] R. J. Mustafa, and Y. L. Nimir, to be submitted to the J. Composite Materials.

Received April 4, 2001
Accepted December 25, 2001